Power Iteration Clustering

Frank Lin
Carnegie Mellon University
Pittsburgh, PA 15213
frank@cs.cmu.edu

William W. Cohen
Carnegie Mellon University
Pittsburgh, PA 15213
wcohen@cs.cmu.edu

Abstract

We show that the power iteration, or the power method, typically used to approximate the dominant eigenvector of a matrix, can be applied to a normalized affinity matrix to create a one-dimensional embedding of the underlying data. This embedding is then used, as in spectral clustering, to cluster the data via k-means. We demonstrate this method's effectiveness and scalability on several synthetic and real datasets, and conclude that to find a meaningful low-dimensional embedding for clustering, it is *not* necessary to find *any* eigenvector—we just need a good linear combination of the top eigenvectors.

1 Introduction

Spectral clustering is an effective and elegant clustering method based on the pairwise similarity between objects. Here we present a fast and simple spectral-clustering like technique called *power iteration clustering*. As in spectral clustering, points are embedded in a low-dimensional subspace derived from the similarity matrix for the data points; however, while in spectral clustering, the subspace is derived from the bottom eigenvectors of the Laplacian of an affinity matrix, in our proposed method, the subspace is an approximation to a linear combination of these eigenvectors.

We show that our method obtains comparable or better clusters than existing spectral methods; however, the most important advantages of the method are its simplicity and scalability. In particular, the subspace we use is a one-dimensional subspace formed by using the power iteration *with early stopping* on a normalized affinity matrix (the power iteration is normally run to convergence in order to find the dominant eigenvector of a matrix); this technique is simple, scalable, easily parallelized, and quite well-suited to very large datasets.

2 Power iteration clustering

2.1 Notation and background

Given a dataset $X = \{\mathbf{x}_1, \mathbf{x}_2, ..., \mathbf{x}_n\}$, a *similarity function* $s(\mathbf{x}_i, \mathbf{x}_j)$ is a function where $s(\mathbf{x}_i, \mathbf{x}_j) = s(\mathbf{x}_j, \mathbf{x}_i)$ and $s \geq 0$ if $i \neq j$, and following previous work [13, 10], $s = 0$ if $i = j$. An *affinity matrix* $A \in \mathcal{R}^{n \times n}$ is defined by $A_{ij} = s(\mathbf{x}_i, \mathbf{x}_j)$. The *degree matrix* D associated with A is a diagonal matrix with $d_{ii} = \sum_j Aij$. A *normalized affinity matrix* W is defined as $D^{-1}A$. Below we will view W interchangeably as a matrix, and a bidirectional graph with nodes X, and the edges from x_i, x_j weighted by $s(\mathbf{x}_i, \mathbf{x}_j)$.

W is closely related to the *normalized random-walk Laplacian* matrix L of Meilă and Shi [9], which is defined as $L = I - D^{-1}A$. L has a number of useful properties: most importantly to this paper, the second-smallest eigenvector of L (the eigenvector with the second-smallest eigenvalue) defines a partition of the graph W that approximately maximizes the *Normalized Cut* criteria [9]. More generally, the k smallest eigenvectors define a subspace where the clusters are well-separated. Thus the second-smallest, third-smallest, ..., k^{th} smallest eigenvectors of L are often well-suited for clustering the graph W into k components.

Note that the k *smallest* eigenvectors of L are also the k *largest* eigenvectors of W. One simple method for computing the largest eigenvector of a matrix is *power iteration* (hereafter PI), also called the *power method*. PI is an iterative method, which starts with an arbitrary vector $\mathbf{v}^0 \neq \mathbf{0}$ and repeatedly performs the update

$$\mathbf{v}^{t+1} = cW\mathbf{v}^t$$

where c is a normalizing constant to keep $\mathbf{v}^t$ from getting too large and typically $c = 1/\|W\mathbf{v}^t\|_1$ or $1/\|W\mathbf{v}^t\|_2$. When applied to a *column*-normalized affinity matrix W^T, each iteration simulates a step in a Markov random walk with starting distribution $\mathbf{v}^0$ and transition probability matrix W^T, and $\mathbf{v}^t$ converges to a stable distribution if the graph underlying W^T is non-bipartite. Since the operations are simple (matrix-vector multiplications), fast (if W^T is sparse), space-efficient (only $\mathbf{v}^t$ needs to be stored), parallelizable and easily implemented in a distributed computing environment, power iteration is suitable for sparse, large-scale data—for example, web page ranking in the PageRank algorithm [11].

Unfortunately, PI does not seem to be particularly useful in this setting. While the k smallest eigenvectors of L (equivalently, the largest eigenvectors of W) are in general interesting, the very smallest eigenvector of L (the largest eigenvector of W) is not. To see this, note that since the sum of each row of W is 1, a constant vector transformed by W will never change in direction or magnitude, and is hence a constant eigenvector of W with eigenvalue $\lambda_1 = 1$.

2.2 Power iteration convergence

The central observation of this paper is that, while running PI *to convergence* on W does not lead to an interesting result, the intermediate vectors obtained by PI during the convergence process are extremely interesting. This is best illustrated by example. Figure 1(a) shows a simple dataset—i.e., each $\mathbf{x}_i$ is a point in $\mathcal{R}^2$ space, with $s(\mathbf{x}_i, \mathbf{x}_j)$ defined as $exp\left(\frac{-\|\mathbf{x}_i - \mathbf{x}_j\|^2}{2\sigma^2}\right)$. Figures 1(b) to 1(h) shows $\mathbf{v}^t$ at various values of t, each illustrated by plotting $\mathbf{v}^t(i)$ for each $\mathbf{x}_i$.[1]

Qualitatively, PI first converges *locally* within a cluster: by $t = 600$ the points from each cluster have approximately the same value in $\mathbf{v}^t$, leading to three disjoint line segments in the visualization. Then, after local convergence, the line segments draw closer together more slowly.

This behavior can be understood by recognizing that PI is a sort of iterative averaging. Variants of iterative averaging are often used to propagate class label information through the graph in graph-based semi-supervised learning methods (e.g., [18], [8], [3, 14]). For PI, at each iteration, an element i in $\mathbf{v^t}$ is updated to $\mathbf{v^t}(i) \leftarrow \frac{1}{c}\sum_j W_{ij}\mathbf{v^{t-1}}(j)$ where c is some constant; this means that the element i is set to a weighted average of its neighbors in the underlying graph weighted according to W_{ij}. If the underlying graph is connected, repeated averaging will eventually make all nodes have the same value; however, sets of nodes that are near each other will quickly attain a similar value, while nodes that are far away in the graph will converge in value more slowly.

2.3 Analysis of PI's convergence rate

Let us assume that W has eigenvectors $\mathbf{e}_1, \ldots, \mathbf{e}_n$ with eigenvalues $\lambda_1, \ldots, \lambda_n$, where $\lambda_1 = 1$ and $\mathbf{e}_1$ is constant. Given W, we define the *spectral representation* of a value $a \in \{1, \ldots, n\}$ to be the vector $\mathbf{s}_a = \langle \mathbf{e}_1(a), \ldots, \mathbf{e}_k(a) \rangle$, and define the *spectral distance between a and b* as

$$spec(a, b) \equiv \|\mathbf{s}_a - \mathbf{s}_b\|_2 = \sqrt{\sum_{i=2}^{k} (\mathbf{e}_i(a) - \mathbf{e}_i(b))^2}$$

[1]For purposes of visualization, the instances $\mathbf{x}$ in the "bulls-eye" are ordered first, followed by instances in the central ring, followed by instances in the outer ring. We have also re-scaled the plots to span the same vertical distance—in reality the differences between the distinct values of the $\mathbf{v^t}(i)$'s become smaller as t increases.

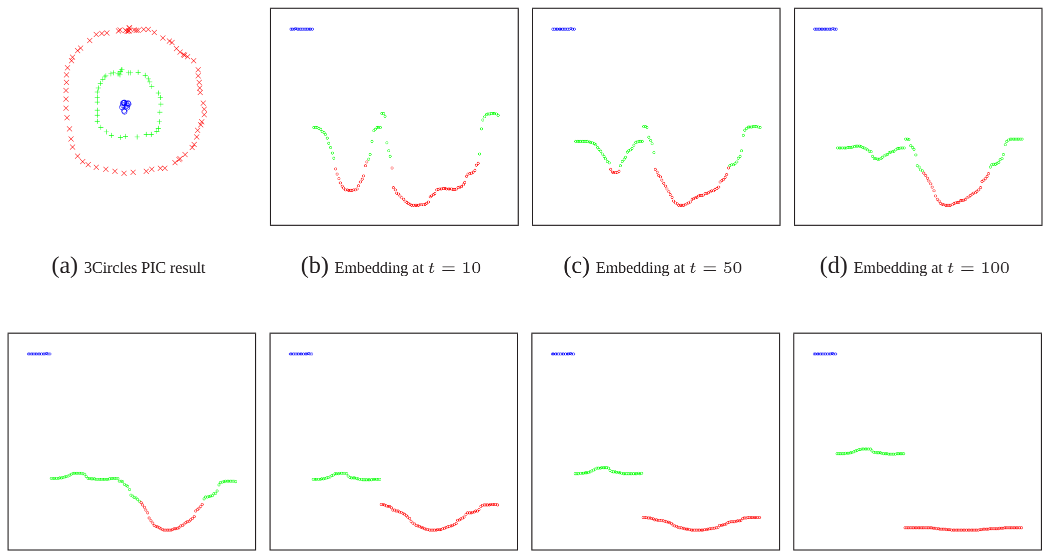

(a) 3Circles PIC result (b) Embedding at $t = 10$ (c) Embedding at $t = 50$ (d) Embedding at $t = 100$

(e) Embedding at $t = 200$ (f) Embedding at $t = 400$ (g) Embedding at $t = 600$ (h) Embedding at $t = 1000$

Figure 1: Clustering result and the embedding provided by $\mathbf{v}^t$ for the 3Circles dataset. In (b) through (h), the value of each component of $\mathbf{v}^t$ is plotted against its index.

Usually in spectral clustering it is assumed that the eigenvalues $\lambda_2, \ldots, \lambda_k$ are larger than the remaining ones. We define W to have an (α, β)*-eigengap between the* k^{th} *and* $(k+1)^{th}$ *eigenvector* if $\lambda_k/\lambda_2 \geq \alpha$ and $\lambda_{k+1}/\lambda_2 \leq \beta$. We will also say that W is γ_e*-bounded* if $\forall i, a, b \in \{1, \ldots, n\}$, $|\mathbf{e}_i(a) - \mathbf{e}_i(b)| \leq \gamma_e$; note that every W is γ_e-bounded for some γ_e. Letting $\mathbf{v}^t$ be the result of of the t^{th} iteration of PI, we define the $(t, \mathbf{v}^0)$*-distance between* a *and* b as

$$pic^t(\mathbf{v}^0; a, b) \equiv |\mathbf{v}^t(a) - \mathbf{v}^t(b)|$$

We will say that $\mathbf{v}^0$ is (c_{lo}, c_{hi})*-bounded* if $\mathbf{v}^0 = c_1\mathbf{e}_1 + \ldots + c_n\mathbf{e}_n$ and $\forall i \in \{1, \ldots, n\}$, $c_{lo} \leq c_i \leq c_{hi}$. For brevity, we will usually drop $\mathbf{v}^0$ from our notation (e.g., writing $pic^t(a, b)$) but assume that $\mathbf{v}^0$ is (c_{lo}, c_{hi})-bounded.

Our goal is to relate $pic^t(a, b)$ and $spec(a, b)$. Let us first define

$$signal^t(a, b) \equiv \sum_{i=2}^{k} [\mathbf{e}_i(a) - \mathbf{e}_i(b)] c_i \lambda_i^t$$

$$noise^t(a, b) \equiv \sum_{j=k+1}^{n} [\mathbf{e}_j(a) - \mathbf{e}_j(b)] c_j \lambda_j^t$$

Proposition 1. *For any* W *with* $\mathbf{e}_1$ *a constant vector,*

$$pic^t(a, b) = |signal^t(a, b) - noise^t(a, b)|$$

To verify the proposition, note that (ignoring renormalization)

$$\begin{aligned} \mathbf{v}^t &= W\mathbf{v}^{t-1} = W^2\mathbf{v}^{t-2} = \ldots = W^t\mathbf{v}^0 \\ &= c_1 W^t \mathbf{e}_1 + c_2 W^t \mathbf{e}_2 + \ldots + c_n W^t \mathbf{e}_n \\ &= c_1 \lambda_1^t \mathbf{e}_1 + c_2 \lambda_2^t \mathbf{e}_2 + \ldots + c_n \lambda_n^t \mathbf{e}_n \end{aligned}$$

Rearranging terms,

$$pic^t(a, b) = \left| [\mathbf{e}_1(a) - \mathbf{e}_1(b)] c_1 \lambda_1^t + \sum_{i=2}^{k} [\mathbf{e}_i(a) - \mathbf{e}_i(b)] c_i \lambda_i^t + \sum_{j=k+1}^{n} [\mathbf{e}_j(a) - \mathbf{e}_j(b)] c_j \lambda_j^t \right|$$

where the second and third terms correspond to $signal^t$ and $noise^t$ respectively, and the first term is zero because $\mathbf{e}_1$ is a constant vector.

The implications of this are somewhat clearer if we define a "radius" $R^t \equiv \frac{1}{c_{lo}\lambda_2^t}$ and consider the product of R^t and the quantities above. Clearly

$$R^t noise^t(a,b) \leq (n-k)\gamma_e \frac{c_{hi}}{c_{lo}}\beta^t$$
$$R^t signal^t(a,b) = \sum_{i=2}^{k}[\mathbf{e}_i(a) - \mathbf{e}_i(b)]\frac{c_i}{c_{lo}}\left(\frac{\lambda_i}{\lambda_2}\right)^t$$

So, after rescaling points by R^t, we see that $noise^t$ will shrink quickly, if the β parameter of the eigengap is small. We also see that $signal^t$ is some sort of approximate version of $spec$: the differences that that $signal^t$ is (a) compressed to the small radius R^t (b) has components distorted by factors of $\frac{c_i}{c_{lo}}\left(\frac{\lambda_i}{\lambda_2}\right)^2$ and (c) has terms that are additively combined (rather than combined with Euclidean distance). Note that the size of the radius is of no importance in clustering; also, if the first few eigenvalues are close to one (i.e., α is large) and c_{lo} is not too small, the distorting factors are bounded. We are left with the problem that the term in the sum defining $signal^t$ are additively combined.

We can make a much stronger connection between $signal^t$ and $spec$ if we are willing to assume more about W. More precisely, let a *clustering* cl for W be a function $cl : \{1,\ldots,n\} \to \{2,\ldots,k\}$. Meilă and Shi [9] note that for many natural problems, W is approximately block-stochastic, and the first few non-dominant eigenvectors are approximately piecewise constant over clusters. To formalize this, define W to be $(\gamma_{cl},\delta_{cl})$-*clusterable* if there is a clustering cl such that

1. $\forall a,b$ if $cl(a) = cl(b)$ then
$$\forall i : 2 \leq k, |\mathbf{e}_i(a) - \mathbf{e}_i(b)| \leq \delta_{cl}$$
2. $\forall a,b$ if $cl(a) \neq cl(b)$ then there is some $i : 2 \leq i \leq k$ such that
$$|\mathbf{e}_i(a) - \mathbf{e}_i(b)| \geq \gamma_{cl}$$
$$\forall j \neq i, 1 \leq j \leq n, |\mathbf{e}_j(a) - \mathbf{e}_j(b)| \leq \delta_{cl}$$

The immediate implication of this is that $spec(a,b)$, whenever it is large, is the result of a large difference in a single eigenvector, which means that summing the differences between the individual eigenvectors at a and b is a good approximation. We have the following result.

Theorem 1. *If W is $(\gamma_{cl},\delta_{cl})$-clusterable and has an (α,β)-eigengap, then*

- *If $cl(a) \neq cl(b)$, then $spec(a,b) \geq \gamma_{cl}$ and $R^t signal^t(a,b) \geq \gamma_{cl}\alpha^t - (k-2)\frac{c_{hi}}{c_{lo}}\delta_{cl}$*
- *If $cl(a) = cl(b)$, then $spec(a,b) \leq \sqrt{(k-1)\delta_{cl}^2}$ and $R^t signal^t(a,b) \leq (k-1)\frac{c_{hi}}{c_{lo}}\delta_{cl}$*

Hence for large enough α and γ_{cl}, small enough t, and small enough δ_{cl}, $signal^t$ is a good approximation of $spec$. It additionally β is small enough, and t is large enough, then $noise^t$ goes to zero faster than $signal^t$. This suggest that for some values of t, $pic^t(a,b)$ will be a good approximation of $spec(a,b)$.

2.4 Clustering based on PI with early stopping

These observations suggest that an effective clustering algorithm might run PI for some number of iterations t, stopping when $\mathbf{v}^t$ becomes a useful linear combination of the first k eigenvectors, followed by clustering the eigenvalues of $\mathbf{v^t}$. If we are able to detect and stop PI *after* it has converged within cluster but *before* the entire dataset converges, we will have an approximately piecewise constant vector, where the elements that are in the same cluster having similar values.

Our stopping heuristic is based on the assumption and observation that while the clusters are "locally converging", the rate of convergence also changes rapidly; whereas during the final global convergence, the converge rate appears more stable. This assumption turns out to be well-justified; recall

```
Input: A row-normalized affinity matrix $W$ and the number of clusters $k$.
Output: Clusters $C_1, C_2, ..., C_k$.
    1. Pick an initial vector $\mathbf{v^0}$.
    2. Set $\mathbf{v^{t+1}} \leftarrow \frac{W\mathbf{v^t}}{\|W\mathbf{v^t}\|_1}$ and $\boldsymbol{\delta}^{t+1} \leftarrow |\mathbf{v^{t+1}} - \mathbf{v^t}|$.
    3. Increment $t$ and repeat above step until $|\boldsymbol{\delta}^t - \boldsymbol{\delta}^{t-1}| \simeq \mathbf{0}$.
    4. Use $k$-means to cluster points on $\mathbf{v^t}$ and return clusters $C_1, C_2, ..., C_k$.
```

Figure 2: The PIC algorithm.

that $\mathbf{v}^t = c_1\lambda_1^t\mathbf{e}_1 + c_2\lambda_2^t\mathbf{e}_2 + ... + c_n\lambda_n^t\mathbf{e}_n$. Then

$$\frac{\mathbf{v}^t}{c_1\lambda_1^t} = \mathbf{e}_1 + \frac{c_2}{c_1}\left(\frac{\lambda_2}{\lambda_1}\right)^t \mathbf{e}_2 + ... + \frac{c_n}{c_1}\left(\frac{\lambda_n}{\lambda_1}\right)^t \mathbf{e}_n$$

It is then evident that the convergence rate of PI towards the dominant eigenvector $\mathbf{e}_1$ depends on $(\lambda_i/\lambda_1)^t = (\lambda_i/1)^t$. For the significant terms $2, ..., k$, since their eigenvalues are close to 1 if the clusters are well-separated [9, 15] $(\lambda_i/1)^t \simeq 1$. This implies that in the beginning of PI, it converges towards a linear combination of the top k eigenvectors, with terms $k+1, \ldots, n$ diminishing at a rate of $\geq (\lambda_{k+1}/1)^t$. After the noise terms $k+1, \ldots, n$ go away, the convergence rate towards $\mathbf{e}_1$ becomes nearly constant.

Specifically, define the *velocity at* t to be the vector $\boldsymbol{\delta}^t = \mathbf{v}^t - \mathbf{v}^{t-1}$ and define the *acceleration at* t to be the vector $\boldsymbol{\epsilon}^t = \boldsymbol{\delta}^{\mathbf{t}} - \boldsymbol{\delta}^{\mathbf{t-1}}$. We pick a small threshold $\hat{\epsilon}$ and stop PI when $\|\boldsymbol{\epsilon}^t\|_\infty \leq \hat{\epsilon}$. In all experiments in this paper, we let $\hat{\epsilon} = \frac{1\times10^{-5}}{n}$ where n is the number of data instances. The complete algorithm, which we call power iteration clustering, is shown in Figure 2.

Two issues remain to discuss: the details of the k-means clustering method and the choice of a starting point. In practice, k-means converges very fast but is sensitive to the random initial centers and can get stuck in local minima. To avoid this, we run k-means several times and keep track of the within-cluster sum of squares (hereafter WCSS) and use the result with the smallest WCSS. Multiple trials of k-means is very cheap for PIC since distances are calculated in a one-dimension space. 10 k-means trials are used in all the experiments reported in the following section.

The convergence trajectory for PI will be the similar for any initial vector $\mathbf{v^0}$ (other than constant vectors, which multiples of the actual top eigenvector to which PI will converge.) However, we found it useful to let $\mathbf{v^0}(i)$ be $\frac{\sum_j Aij}{V(A)}$, where $V(A)$ is the volume of the affinity matrix A and $V(A) = \sum_i \sum_j Aij$. Since for each element in this vector also correspond to the degree distribution of the graph underlying the affinity matrix A, we will also call this vector a *degree vector* $\mathbf{d}$. The degree vector is the dominant eigenvector of W^T, i.e., the steady distribution of a Markov random walk with W^T, rather than W, as the transition matrix. In some sense, then, this vector is “very distant” from the dominant eigenvector of W. The degree vector also gives more initial weight to the high-degree nodes in the underlying graph, which means that, in the averaging view, values will be distributed more evenly and quickly, leading to faster local convergence.

3 Experiments

3.1 Behavior on synthetic datasets

Figure 3 shows the clustering results of PIC and the one-dimension PIC embedding on several synthetic datasets. The instances in these datasets lie on a 500-by-500 2-dimension plane and $\mathbf{x}_i$ in a dataset X has the x- and y-coordinates as its two components. The affinity matrix A is defined by $A_{ij} = exp\left(\frac{-||\mathbf{x}_i - \mathbf{x}_j||^2}{2\sigma^2}\right)$ and σ^2 is set to 200. The colors in the clustering results correspond to the colors in the embedding; for the embedding the value of the elements of $\mathbf{v^t}$ is plotted against its index, and instances in the same cluster are indexed consecutively. Note that clusters that are closer to each other in the original data generally are also embedded near each other (e.g., Figure 3(h)).

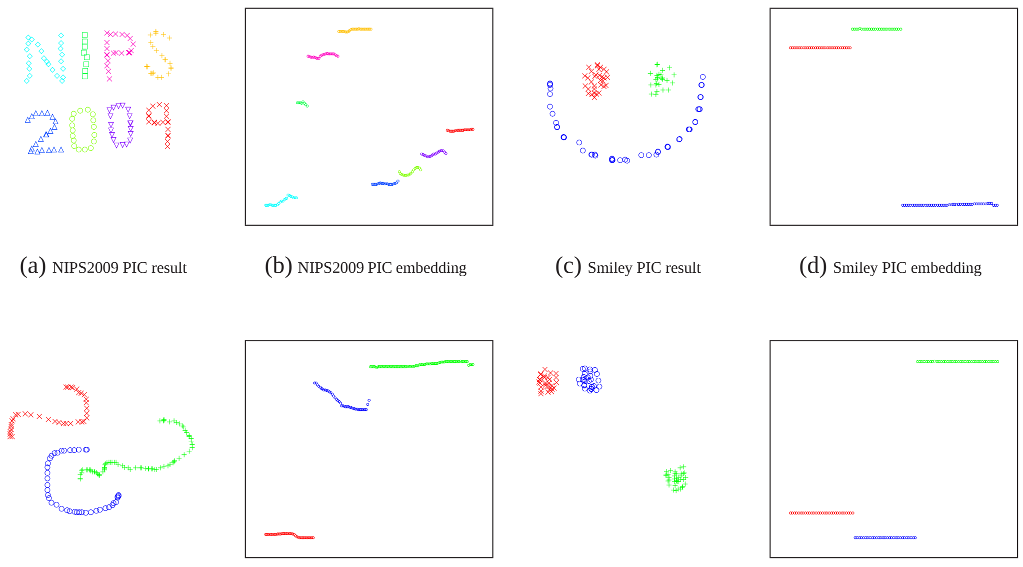

(a) NIPS2009 PIC result (b) NIPS2009 PIC embedding (c) Smiley PIC result (d) Smiley PIC embedding

(e) Squiggles PIC result (f) Squiggles PIC embedding (g) 3Blobs PIC result (h) 3Blobs PIC embedding

Figure 3: Power iteration clustering results on synthetic datasets.

3.2 Accuracy on real datasets

We also demonstrate the effectiveness of PIC on several real datasets from various domains. These datasets have known labels and are mainly used for classification tasks:

- **Iris** is a dataset where features are flower petal and sepal measurements from three species of irises, two of which are not linearly separable from each other. It contains 150 instances total, 50 per species.
- **PenDigits01** and **PenDigits17** are hand-written digit datasets, containing the digits "0", "1" and "1", "7", respectively. Each dataset contains 200 instances, 100 per digit, randomly chosen from roughly 1000 instances by 44 writers. **PenDigits01** represents an "easy" dataset and **PenDigits17** represents a "difficult" dataset since the latter two digits are more difficult to differentiate in hand writing.
- **UBMCBlog** is a connected network dataset of 404 liberal and conservative political blogs as described in [6]. The dataset has no textual features and contains only link structure mined from posts of these blogs in a month's time; i.e., blog a is linked to blog b if a has a post containing a hypertext link to a post in b.)
- **AGBlog** is a connected network dataset of 1222 liberal and conservative political blogs as described in [1]. The dataset has no textual features and contains only link structure mined mostly from the "sidebars"; i.e., it represents a social network of the blogs.
- **20ng*** datasets are subsets of the 20 newsgroups text dataset. **20ngA** contains 100 documents from 2 newsgroups: *misc.forsale* and *soc.religion.christian*. **20ngB** adds an additional 100 documents to each group from **20ngA**. **20ngC** adds 200 documents from *talk.politics.guns* to **20ngB**. **20ngD** adds 200 documents from *rec.sport.baseball* to **20ngC**.

Here we use these labeled datasets for clustering and evaluate the clustering results as classification results in the following way: for a cluster C returned by a clustering algorithm, the true labels of instances within C are revealed and counted, and the entire cluster is assigned the label of with the highest count. Then the resulting labels from the entire dataset is evaluated according to the standard accuracy and macro-averaged F1 measure used for classification tasks.

		NCut		NJW		PIC	
Dataset	**k**	**Accuracy**	**Macro-F1**	**Accuracy**	**Macro-F1**	**Accuracy**	**Macro-F1**
Iris	3	0.673	0.570	0.807	0.806	0.980	0.980
PenDigits01	2	1.000	1.000	1.000	1.000	1.000	1.000
PenDigits17	2	0.755	0.753	0.755	0.754	0.755	0.753
UBMCBlog	2	0.953	0.953	0.953	0.953	0.948	0.948
AGBlog	2	0.520	0.342	0.520	0.342	0.957	0.957
20ngA	2	0.955	0.955	0.955	0.955	0.960	0.960
20ngB	2	0.505	0.344	0.550	0.436	0.905	0.904
20ngC	3	0.613	0.621	0.635	0.639	0.737	0.730
20ngD	4	0.469	0.432	0.535	0.534	0.580	0.570
Average	-	0.716	0.663	0.746	0.713	0.869	0.867

Table 1: Clustering performance of PIC and spectral clustering algorithms on several real datasets.

For the network datasets (**UBMGBlog**, **AGBlog**), the affinity matrix is simply $A_{ij} = 1$ if blog i has a link to j or vice versa, otherwise $A_{ij} = 0$. For all other datasets, the affinity matrix is simply the cosine similarity between feature vectors: $\frac{\mathbf{x}_i \cdot \mathbf{x}_j}{\|\mathbf{x}_i\|_2 \|\mathbf{x}_j\|_2}$. Cosine similarity is used instead of the distance function in Section 3.1 to avoid having to tune σ^2. For the text datasets (**20ng***), word counts are used as feature vectors with only stop words and singleton words removed.

We also compare the results of PIC against spectral clustering methods Normalized Cuts (NCut) [13, 9] and NJW [10] and present the results in Table 1. Note that in all cases PIC does better than (**Iris, AGBlog, 20ngA, 20ngB, 20ngC**) or is competitive with the other algorithms. In the case where NCut or NJW fails badly (**AGBlog, 20ngB**), the most likely cause is that the top k eigenvectors of the graph Laplacian fail to provide a good low-dimensional embedding for k-means. Additional algorithms and heuristics are required to carefully choose the "good" eigenvectors and discard the "bad" eigenvectors [17, 7, 16]. PIC, on the other hand, avoids having to choose among eigenvectors by embedding a weighted combinations of the most informative eigenvectors (not necessarily k) onto a subspace.

3.3 Scalability

		NCut	NJW	PIC	
Dataset	**Size**	**Runtime**	**Runtime**	**Runtime**	**Iterations**
Iris	150	589	242	59	6
PenDigits01	200	965	326	56	6
PenDigits17	200	1197	528	62	6
UBMCBlog	404	4205	1589	85	21
AGBlog	1222	114821	58145	211	34
20ngA	200	1113	355	72	15
20ngB	400	4085	1864	139	13
20ngC	600	13070	6383	190	13
20ngD	800	33191	16295	278	11

Table 2: Runtime comparison (in milliseconds) of PIC and spectral clustering algorithms on several real datasets.

Perhaps one of the greatest advantages of PIC lies in its scalability. Space-wise it needs only a single vector of size n as $\mathbf{v}^t$ and two more of the same to keep track of convergence. Speed-wise, power iteration is known to be fast on sparse matrices and converges fast on many real-world datasets; yet PIC converges even more quickly than PI, since by definition it stops when $\mathbf{v}^t$ is no longer accelerating towards convergence. Table 2 shows the runtime of PIC and the spectral clustering algorithms on some datasets described in the previous section. Note that PIC converges with relatively few iterations, and for datasets with similar properties (**20ng***), fewer iterations are required as dataset size grows. Figure 4(a) and 4(b) plots the runtime data on a log-log scale.

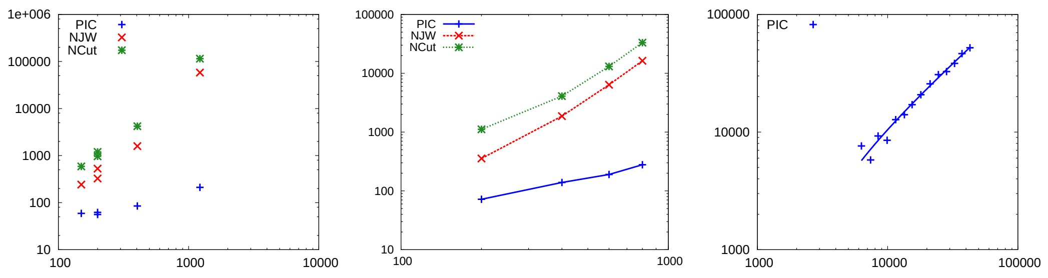

(a) Iris, PenDigits, UBMCBlog & AGBlog (b) 20 Newsgroups (c) Gene Citation

Figure 4: Comparison of algorithm runtime on different datasets. The number of instances is plotted against the runtime in milliseconds on a log-log scale.

In addition to the datasets described, we tested PIC on a large gene citation network dataset, which contains genes that are linked to the papers that mentions them, and papers that are linked to the authors that wrote the papers, and the authors. (For further details see [2]). We run PIC on increasing subsamplings of this dataset, with each subsample adding an additional year of publications, from 1983 to 1996. The largest dataset contains roughly 43,000 nodes and 100,000 edges. The runtime is shown in Figure 4(c) and is linear to the number of nodes.

For these experiments, all algorithms are implements in Java, and for the spectral clustering methods the eigenvectors are calculated via eigenvalue decomposition. Experiments are ran on a single Linux machine with a Intel 1.86GHz CPU and 4GB RAM.

4 Concluding remarks

Spectral clustering began with the discovery of the correlation between the eigenvalues of the Laplacian matrix and the connectivity of a graph [5]. Later it was introduced to the machine learning community through Ratio Cut [12] and Normalized Cuts [13, 9]. Since then it has sparked much interest and lead to further analyses and modifications [10, 15]. Typically, a spectral clustering algorithm defines a Laplacian matrix, such as the row-normalized one in [13] or symmetrically normalized one in [10]. Then the first k smallest eigenvectors, deemed the most informative, are used to embed the data onto a k-dimensional space on which a k-means algorithm is used to obtain the final clusters. However, simply using the first k eigenvectors seems to fail on many real datasets because they often turned out to be uninformative, especially in the presence of noise. This prompted the recent work on selecting "good" eigenvectors and dealing with noisy data [17, 7, 16].

PIC is related to spectral clustering in that eigenvectors play an important role in a low-dimensional embedding of data. PIC also uses k-means on the one-dimension embedding to produce the final clusters. PIC's main advantage is its relative simplicity, and lower computational cost, as it is not necessary to find several eigenvectors. In fact, the experiments show that it is *not* necessary to find *any* eigenvector in order to find a low-dimensional embedding for clustering—the embedding just needs to be a good linear combination of the top eigenvectors.

Another recent graph clustering approach that has shown substantial speed improvement over spectral clustering methods is *multilevel kernel k-means* [4]. In [4], the general *weighted kernel k-means* is shown to be equivalent to a number of spectral clustering methods in its objective when the right weights and kernel matrix are used. Performance wise, spectral clustering methods are slow but tend to get globally better solutions, whereas kernel k-means is faster but get stuck easily in a local minima; [4] exploits this trade-off using a multilevel approach: first an iterative coarsening heuristic is used to reduce the graph to one with $5k$ nodes where k is the number of desired clusters. Then spectral clustering is used on this coarse graph to produce a base clustering, and then the graph and is refined iteratively (to undo the coarsening), and at each refinement iteration the clustering results of the previous iteration is used as the starting point for kernel k-means. Additional point-swapping can be used to further avoid being trapped in local minima. In comparison, while both are extremely fast compared to traditional spectral clustering methods, PIC is a much simpler algorithm, and like spectral clustering methods, it is much less susceptible to being trapped in local minima.

References

[1] Lada Adamic and Natalie Glance. The political blogosphere and the 2004 u.s. election: Divided they blog. In *Proceedings of the WWW-2005 Workshop on the Weblogging Ecosystem*, 2005.

[2] Andrew Arnold and William W. Cohen. Information extraction as link prediction: Using curated citation networks to improve gene detection. In *Proceedings of the AAAI Conference on Weblogs and Social Media*, 2009.

[3] Shumeet Baluja, Rohan Seth, D. Sivakumar, Yushi Jing, Jay Yagnik, Shankar Kumar, Deepak Ravichandran, and Mohamed Aly. Video suggestion and discovery for YouTube: Taking random walks through the view graph. In *Proceeding of the 17th International Conference on World Wide Web*, 2008.

[4] Inderjit S. Dhillon, Yuqiang Guan, and Brian Kulis. Weighted graph cuts without eigenvectors: A multilevel approach. *IEEE Transactions on Pattern Analysis and Machine Intelligence*, 29(11):1944–1957, 2007.

[5] Miroslav Fiedler. Algebraic connectivity of graphs. *Czechoslovak Mathematical Journal*, 23(98):298–305, 1973.

[6] Anubhav Kale, Amit Karandikar, Pranam Kolari, Akshay Java, Tim Finin, and Anupam Joshi. Modeling trust and influence in the blogosphere using link polarity. In *Proceedings of the International Conference on Weblogs and Social Media (ICWSM 2007)*, 2007.

[7] Zhenguo Li, Jianzhuang Liu, Shifeng Chen, and Xiaoou Tang. Noise robust spectral clustering. In *IEEE 11th International Conference on Computer Vision*, 2007.

[8] Sofus A. Macskassy and Foster Provost. Classification in networked data: A toolkit and a univariate case study. *The Journal of Machine Learning Research*, 8.

[9] Marina Meilă and Jianbo Shi. A random walks view of spectral segmentation. In *IEEE International Conference on Artificial Intelligence and Statistics*, 2001.

[10] Andrew Y. Ng, Michael Jordan, and Yair Weiss. On spectral clustering: Analysis and an algorithm. In *Advances in Neural Information Processing Systems 14*, 2002.

[11] Lawrence Page, Sergey Brin, Rajeev Motwani, and Terry Winograd. The PageRank citation ranking: Bringing order to the web. Technical report, Stanford Digital Library Technologies Project, 1998.

[12] Tom Roxborough and Arunabha Sen. Graph clustering using multiway ratio cut. In *Proceedings of Graph Drawing*, pages 291–296, 1997.

[13] Jianbo Shi and Jitendra Malik. Normalized cuts and image segmentation. *IEEE Transactions on Pattern Analysis and Machine Intelligence*, 22(8):888–905, 2000.

[14] Partha Pratim Talukdar, Joseph Reisinger, Marius Paşca, Deepak Ravichandran, Rahul Bhagat, and Fernando Pereira. Weakly-supervised acquisition of labeled class instances using graph random walks. In *Proceedings of the 2008 Conference on Empirical Methods in Natural Language Processing*, 2008.

[15] Ulrike von Luxburg. A tutorial on spectral clustering. *Statistics and Computing*, 17(4):395–416, 2007.

[16] Tao Xiang and Shaogang Gong. Spectral clustering with eigenvector selection. *Pattern Recognition*, 41(3):1012–1029, 2008.

[17] Lihi Zelnik-Manor and Pietro Perona. Self-tuning spectral clustering. In *Advances in Neural Information Processing Systems 17*, 2005.

[18] Xiaojin Zhu, Zoubin Ghahramani, and John Lafferty. Semi-supervised learning using Gaussian fields and harmonic functions. In *The 20th International Conference on Machine Learning*, 2003.